Science Translational Medicine
AAAS

www.sciencetranslationalmedicine.org/cgi/content/full/9/406/eaan3968/DC1

Supplementary Materials for

Nondestructive tissue analysis for ex vivo and in vivo cancer diagnosis using a handheld mass spectrometry system

Jialing Zhang, John Rector, John Q. Lin, Jonathan H. Young, Marta Sans, Nitesh Katta, Noah Giese, Wendong Yu, Chandandeep Nagi, James Suliburk, Jinsong Liu, Alena Bensussan, Rachel J. DeHoog, Kyana Y. Garza, Benjamin Ludolph, Anna G. Sorace, Anum Syed, Aydin Zahedivash, Thomas E. Milner, Livia S. Eberlin*

*Corresponding author. Email: liviase@utexas.edu

Published 6 September 2017, *Sci. Transl. Med.* **9**, eaan3968 (2017)
DOI: 10.1126/scitranslmed.aan3968

The PDF file includes:

Other Supplementary Material for this manuscript includes the following:
(available at www.sciencetranslationalmedicine.org/cgi/content/full/9/406/eaan3968/DC1)

Movie S1 (.mov format). Simulation demonstrating the use of the MasSpec Pen for routine intraoperative diagnosis.

Materials and Methods

Fabrication of the MasSpec pen tips

The negative molds used to cast the elastomer pen tips were designed using SolidWorks computer aided design (CAD) software and then fused deposition modeled with the 3D printer using ABS plastic (Stratasys) and soluble support material. The parts were then washed to remove support material, using a support cleaning apparatus (SCA-1200HT, SCA) and solvent (EcoWorks) at 70 ^{o}C for 24 hrs or until support material was fully dissolved. For the casting, a mixture of PDMS elastomer base and curing agent (Sylgard 184, Dow Corning) were prepared in a weight ratio of 10:1, respectively. The mixture was poured into the 3-D printed molds, cured in an oven (10GCE-LT, Quincy Lab) at 74 ^{o}C for 1 h, and then placed in a closed container with acetone (Fisher Scientific, Waltham, MA, USA) to dissolve. The final washing step had the tips sonicated in acetone to remove any remaining ABS.

Coupling of the MasSpec Pen to the mass spectrometer

To transport the droplet from the pen tip to the mass spectrometer, a PTFE tubing (conduit 3) was directly connected to the metal transfer tube of a Q Exactive hybrid Quadrupole-Orbitrap mass spectrometer (Thermo Fisher Scientific, San Jose, CA). Vaporization and ionization occurs in the inlet region of the mass spectrometer, similar to what has been observed in solvent assisted inlet ionization (*34*), although various connection methods and ionization sources could be adapted for the system. To facilitate experimental assembly, an integrated MS-interface was designed which houses the pinch valves, microcontroller, and tubing to connect the system to the mass spectrometer inlet.

Identification of molecular ions

Tentative assignments of the molecular ions were performed using high mass accuracy measurements for all ions described, as well as tandem MS analysis when the total abundance of the selected parent ion yielded adequate intensity of fragment ions for structural interpretation. These data were interpreted in light of literature reports on fragmentation patterns of lipid species, as well as information available in lipids (http://www.lipidmaps.org/) and metabolite (http://www.hmdb.ca/) databases to derive a proposed identification that presented the lowest mass error and the most reasonable elemental composition and chemical structure. Note that a maximum tolerance of 10 ppm in mass error was used for the proposed identification. **Tables S1-S5** describe the data used to identify all the peaks mentioned in the paper, for mouse brain, human thyroid, human ovarian, human lung and human breast, respectively. Each table contains the proposed identification, the proposed formula, the measured and theoretical *m/z*, the mass error (in ppm), as well as the fragment peaks obtained in MS/MS analyses, when adequate tandem MS

data was achieved. When tandem MS did not yield interpretable information due to low abundance of the parent and/or fragment ions, only mass accuracy was used to yield a tentative identification or a probable elemental composition based on the mass error value for the given *m/z*. Note that for complex lipids, isomerism of the double bonds in the fatty-acid (FA) chains complicates precise structural assignment despite high mass accuracy measurements and tandem MS data, which is why FA chains are tentatively assigned for all lipids described.

Data Analysis

To quantify reproducibility of MasSpec Pen analyses of mouse brain tissue samples, RSD values were calculated using the ratio of the intensities of peaks *m/z* 834.529/*m/z* 885.550. To quantify similarity between two mass spectra profiles, the cosine similarity was calculated. First, peaks were picked from spectra collected in profile mode using the MALDIquant R package. After binning the spectra to *m/z* 0.01 intervals by rounding and restricting the mass range between *m/z* 500 and *m/z* 1000, the agreement between the two spectra was calculated according to their cosine similarity. A value of 1 indicates that the spectra are identical, while a value of 0 indicates that the spectra are completely orthogonal (completely unrelated).

Supplementary Figures

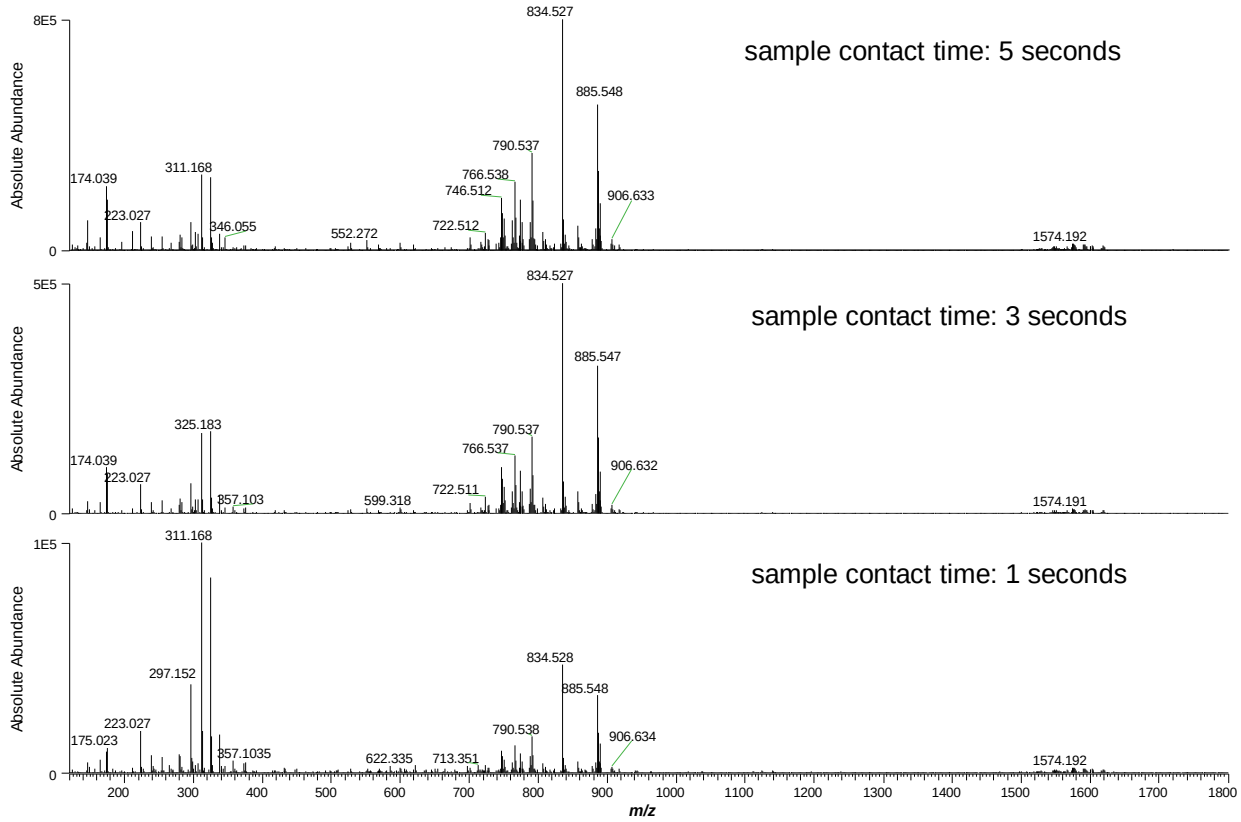

Fig. S1. Effect of MasSpec Pen contact time on the mass spectra obtained. Representative negative ion mode mass spectra obtained from mouse brain tissue sections with different extraction times, 5 s, 3 s, and 1 s (average of n=3 mass spectra each).

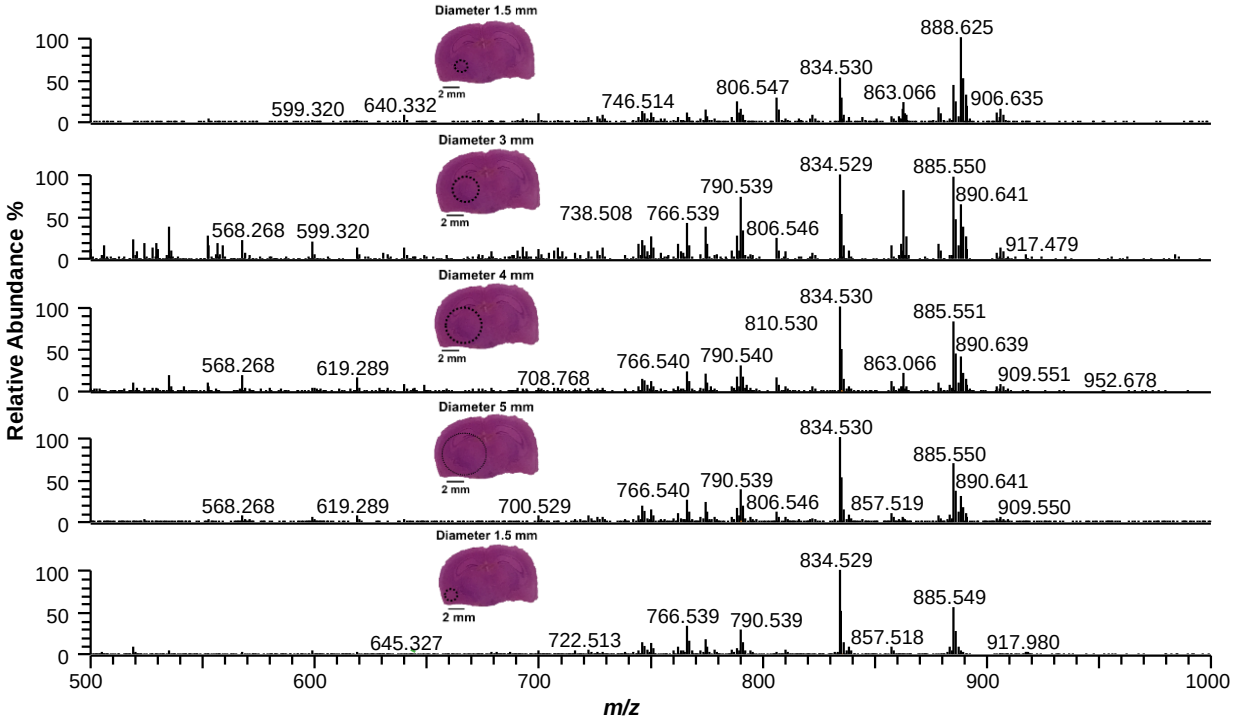

Fig. S2. Effect of MasSpec Pen tip diameter on the mass spectra obtained. Representative negative ion mode mass spectra obtained using several sampling diameters of the MasSpec Pen are shown. Insets show optical images of the H&E stained mouse brain tissue section. The circle in each optical image represents the contact/sampling region where the analysis was performed (average of n=9 mass spectra each).

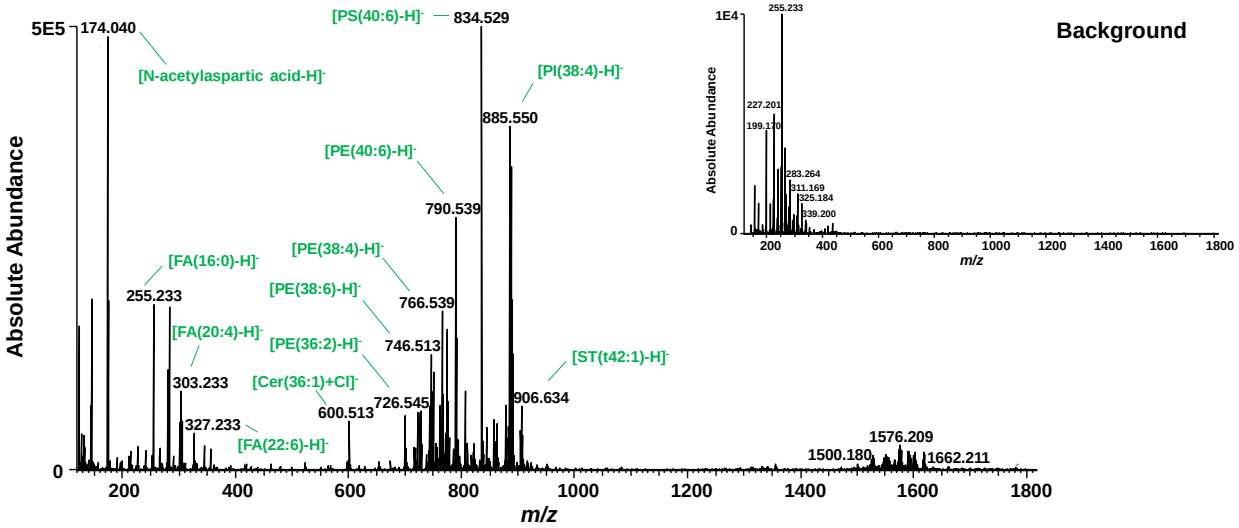

Fig. S3. MasSpec Pen analysis of a mouse brain tissue section. Representative negative ion mode mass spectra from a mouse brain tissue section, and a background region of glass slide (no sample) are shown (average of n=5 mass spectra each).

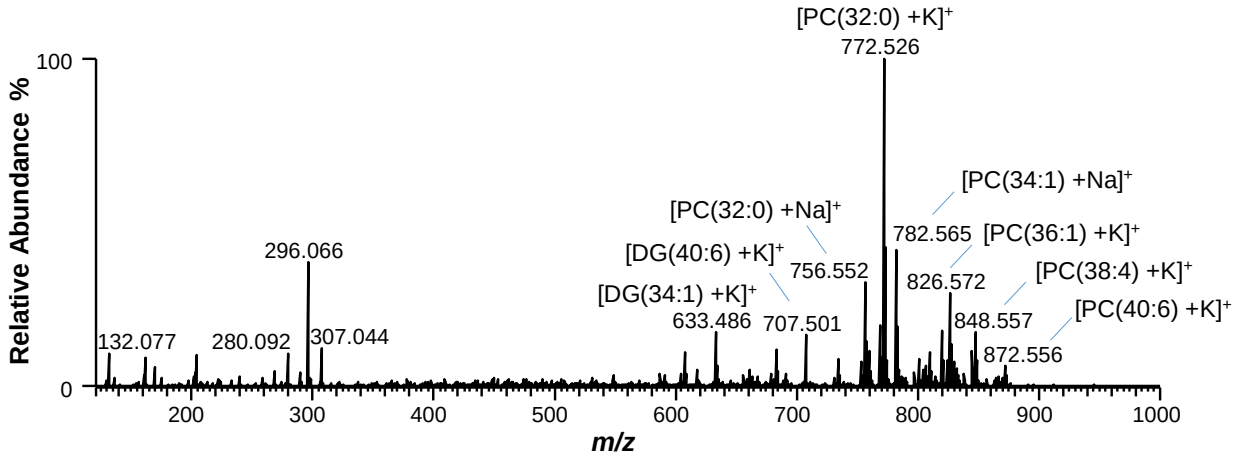

Fig. S4. Positive ion mode analysis using the MasSpec Pen. Representative positive ion mode mass spectrum from a mouse brain tissue section is shown (average of n=3 mass spectra).

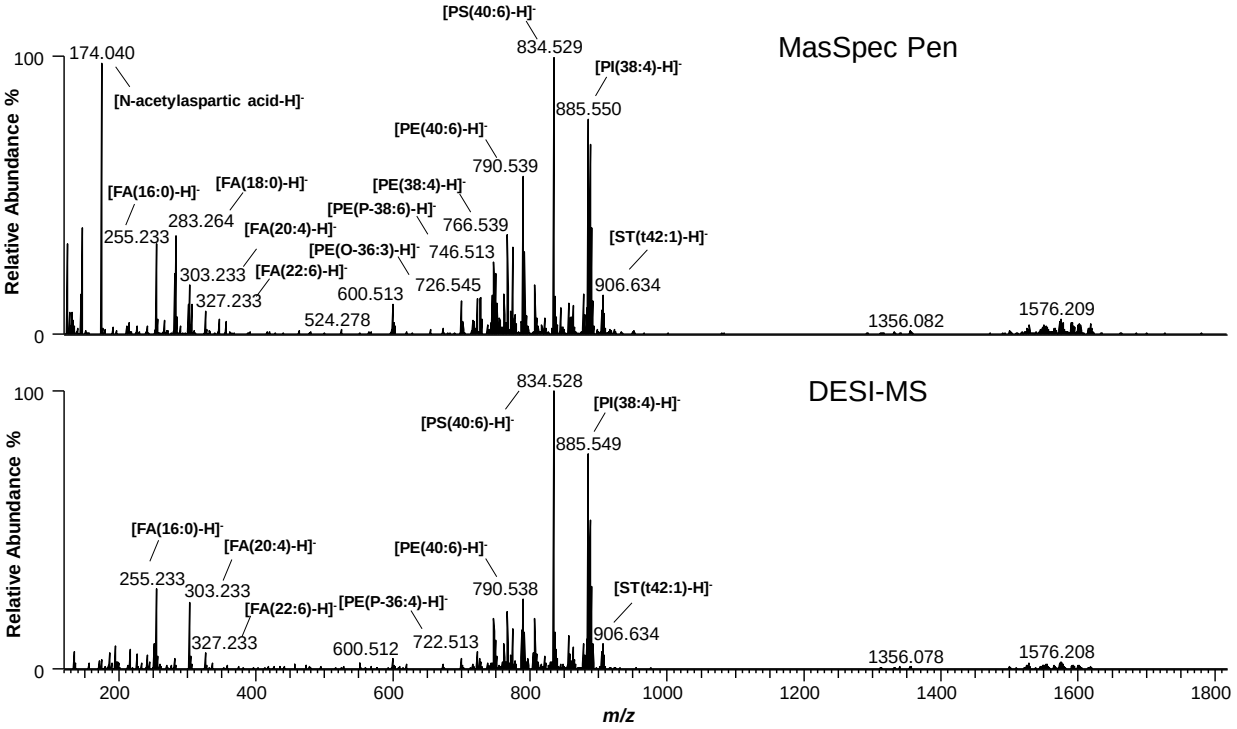

Fig. S5. Comparison between MasSpec Pen and DESI-MSI mass spectra. Negative ion mode MasSpec Pen and DESI mass spectra obtained from a mouse brain tissue section using water as the solvent system are shown (average of n=3 mass spectra each).

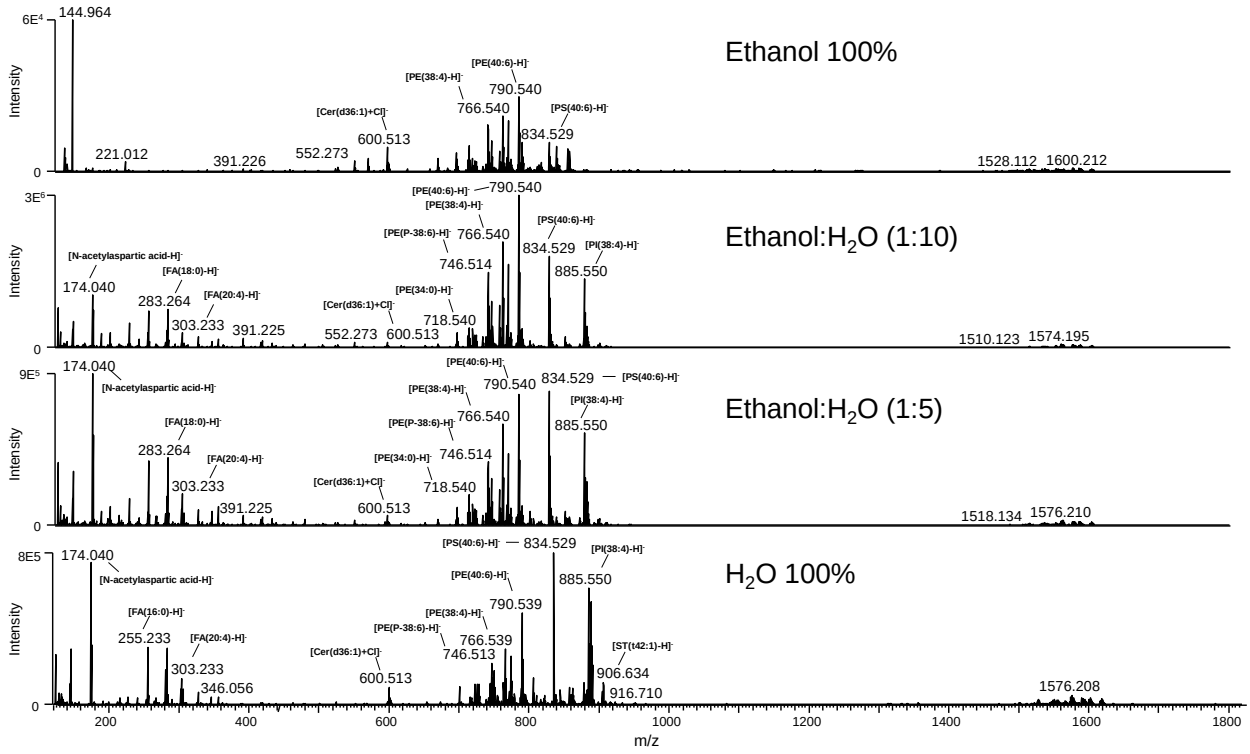

Fig. S6. Effect of MasSpec Pen solvent systems on the mass spectra obtained. Representative negative ion mode MasSpec Pen mass spectra of mouse brain tissue sections obtained using mixtures of water and ethanol at various ratios are shown (average of n=3 mass spectra each).

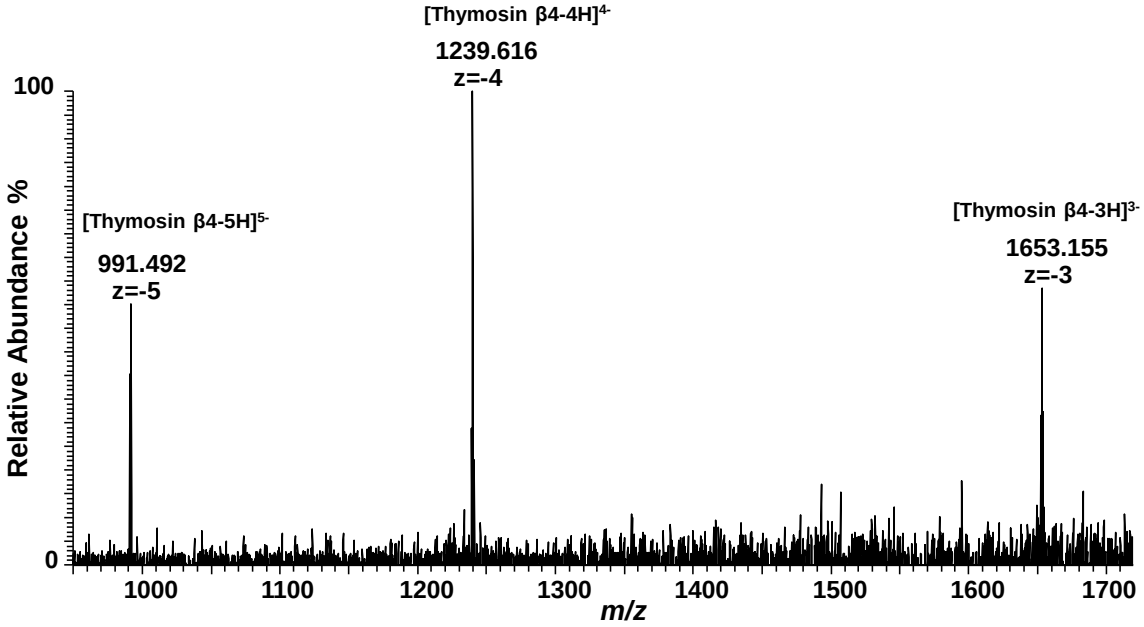

Fig. S7. MasSpec Pen detection of protein ions. Representative negative ion mode mass spectrum from a human breast tissue section shows different charged states detected of a protein tentatively identified as thymosin β-4 (average of n=3 mass spectra).

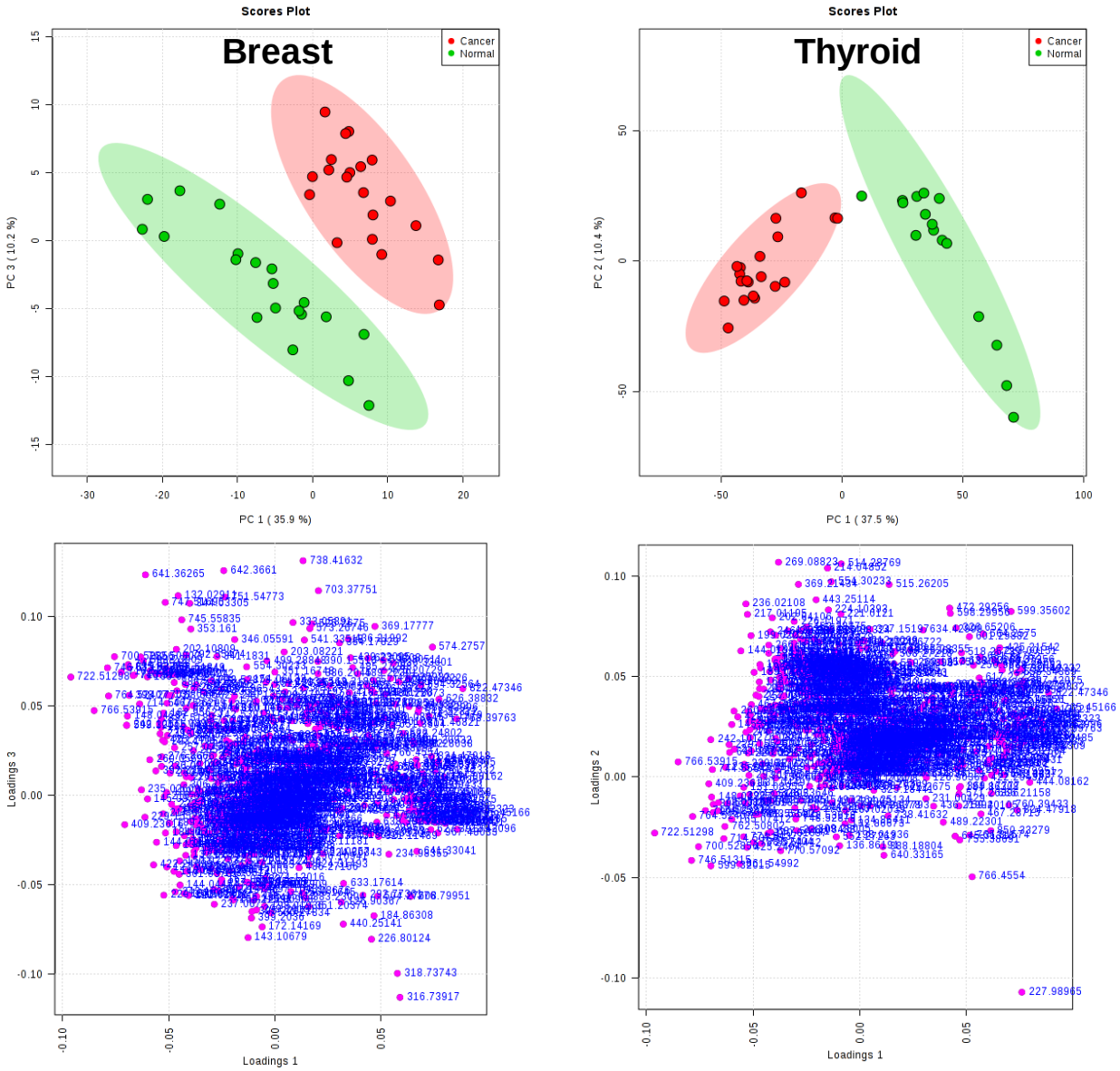

Fig. S8. PCA of the data obtained for the human tissue sections including normal and tumor thyroid and breast tissue sections. Scores plots showing PC1 and PC3 explain 46.1% of the total variance of the breast tissue dataset (left side, n=10 tissue samples), whereas PC1 and PC2 explain 47.9% of the total variance of the thyroid tissue dataset (right side, n=10 tissue samples). Loading plots are also included for each tissue type analyzed.

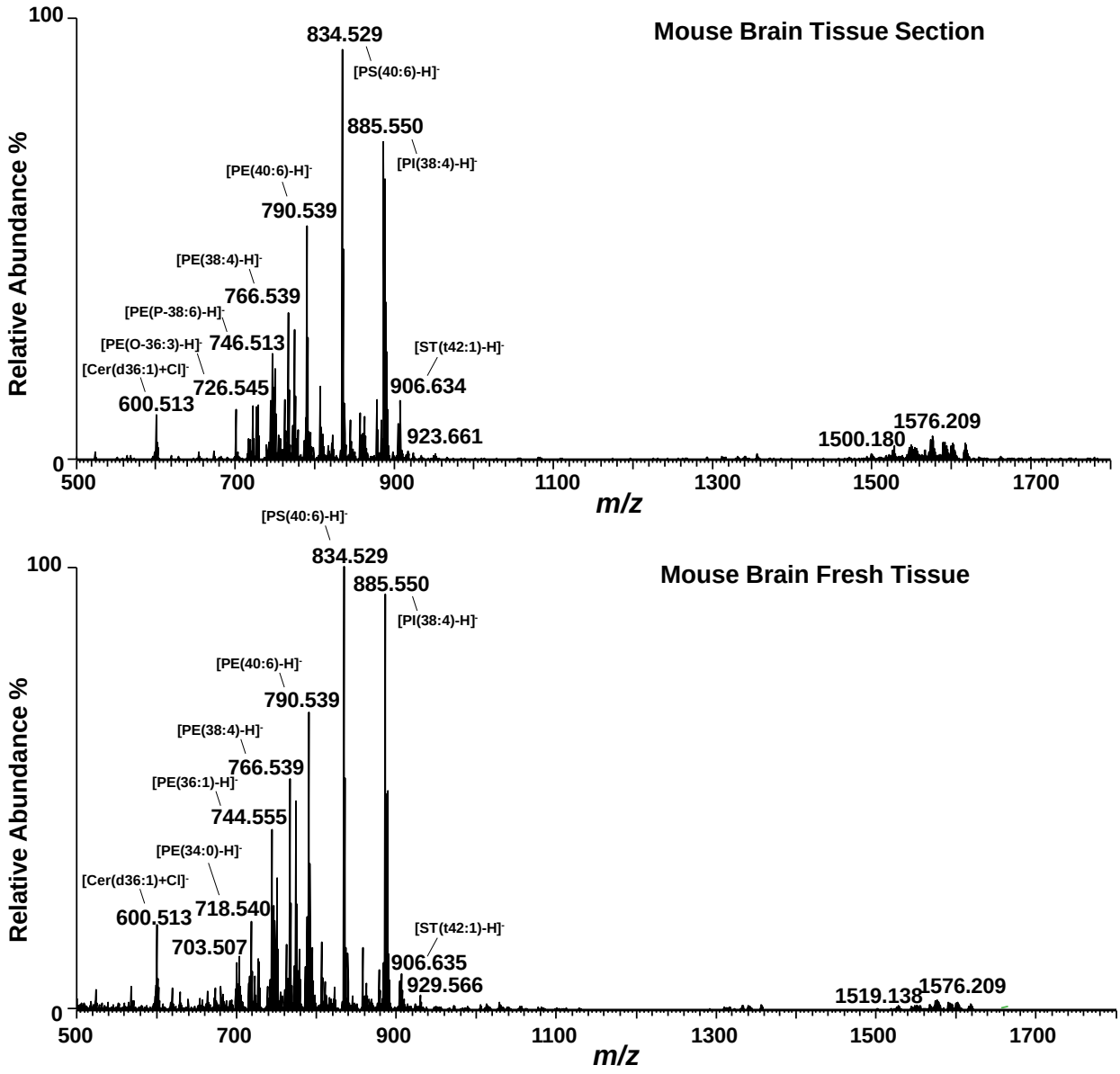

Fig. S9. Comparison between the MasSpec Pen mass spectra obtained from the tissue section and fresh tissue piece. Representative negative ion mode mass spectra of a mouse brain thin tissue section and a mouse brain tissue piece (fresh) analyzed using the MasSpec Pen are shown (fresh, average of n=3 mass spectra each).

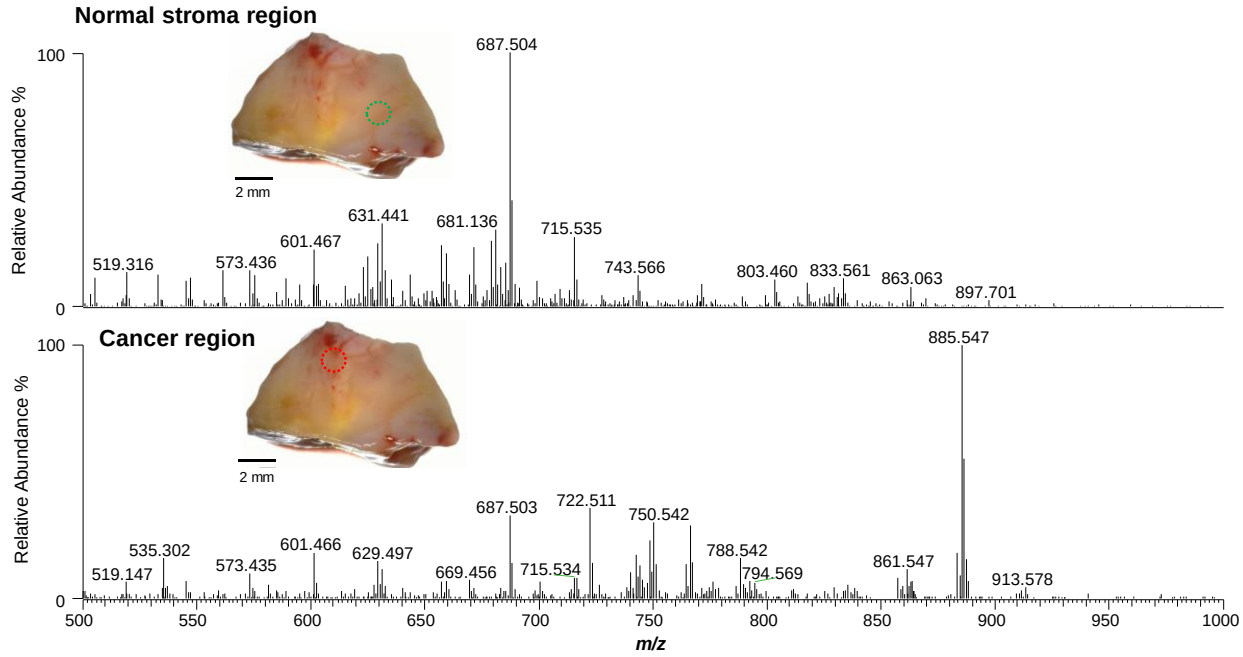

Fig. S10. MasSpec Pen analysis of an HGSC tissue sample with mixed histologic composition. Representative mass spectra obtained from an ovarian tissue sample with normal and cancer tissue regions are shown (average of n=3 mass spectra each). The regions analyzed are delineated over the optical image of the tissue sample using a green dotted circle for the normal ovarian stroma region, and red dotted circle for the ovarian cancer tissue region.

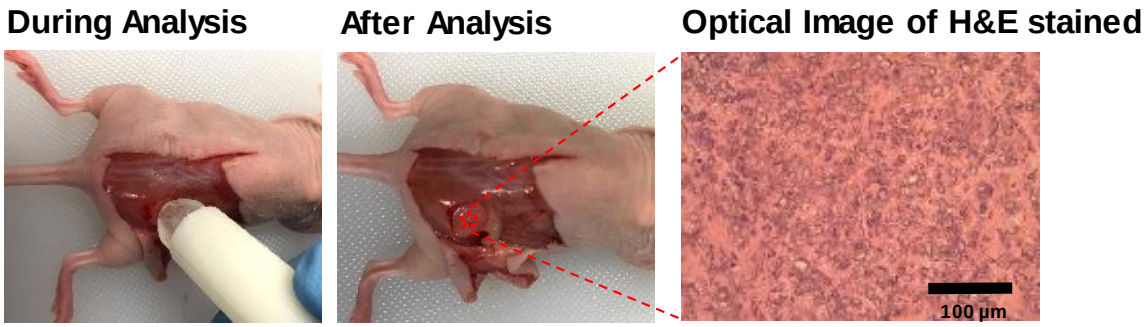

Fig. S11. Intraoperative analysis of tumor and normal tissues in a murine model. Optical and histological images of tissue during and after intraoperative MassSpec pen analysis in a mouse model. The H&E stained tissue section (inset) was obtained from the same region resected after MassSpec Pen analysis.

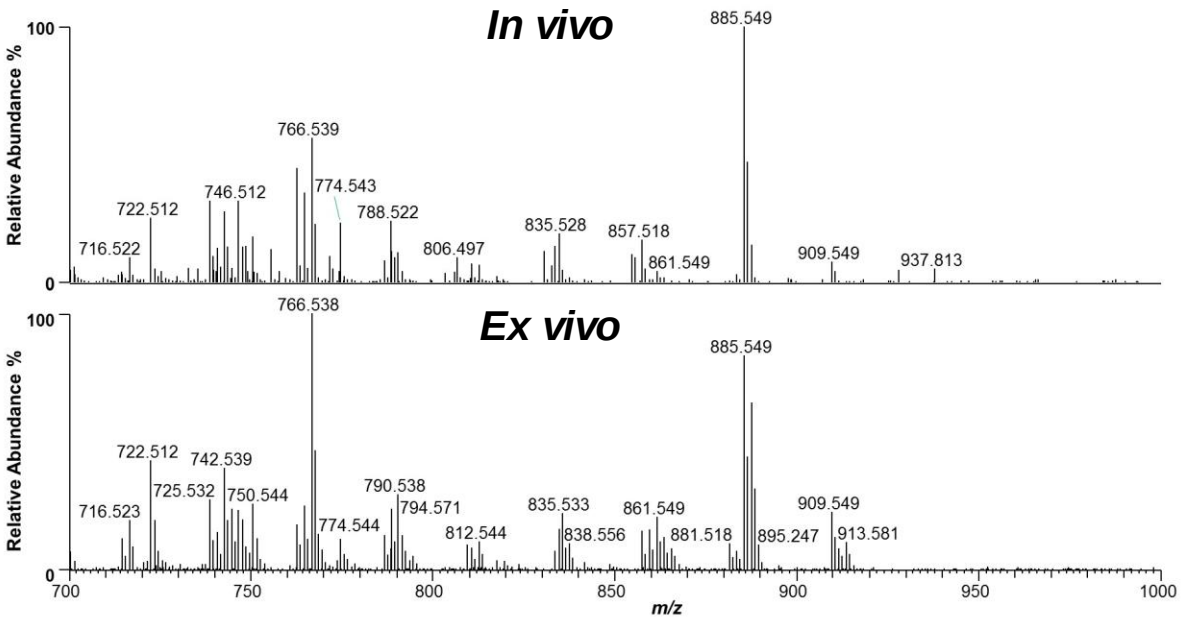

Fig. S12. MasSpec Pen analysis of the same tissue sample in vivo and ex vivo. Representative MasSpec Pen negative ion mode mass spectra obtained *in vivo* and *ex vivo* of the same tumor sample from a mouse model are shown (average of n=3 mass spectra each).

Supplementary Tables

Table S1. Data obtained for the identification of selected negative ion mode molecular ions from mouse brain tissue.

Proposed Identification		Proposed formula	Measured *m/z*	Theoretical *m/z*	Mass error (ppm)	Main Fragment ions upon MS/MS[a]
Thymosin β-4		$C_{212}H_{350}N_{56}O_{78}S_1$	991.091 (-5) 1239.113 (-4) 1652.484 (-3)	991.090 (-5) 1239.114 (-4) 1652.488 (-3)	<1 (-5) <1 (-4) 2.4 (-3)	NA
ST	t42:1	$C_{48}H_{92}NO_{12}S$	906.634	906.635	-1.1	NA
PI	38:4	$C_{47}H_{82}O_{13}P$	885.550	885.550	<1	152.995, 241.011, 283.264, 303.233, 419.257, 581.309
PS	40:6	$C_{46}H_{77}NO_{10}P$	834.529	834.529	<1	152.994, 283.264, 327.233, 419.256, 437.267, 747.497
PE	40:6	$C_{45}H_{77}NO_8P$	790.539	790.539	<1	283.243, 283.264, 327.232, 480.309
	38:4	$C_{43}H_{77}NO_8P$	766.539	766.539	0	259.243, 283.263, 303.232, 480.309
	P-38:6	$C_{43}H_{73}NO_7P$	746.513	746.513	<1	283.243, 327.232, 436.282
	O-36:3	$C_{41}H_{77}NO_7P$	726.545	726.544	1.4	140.010, 152.994, 281.248, 444.288, 462.299
	P-36:4	$C_{41}H_{73}NO_7P$	722.513	722.513	<1	152.994, 259.243, 303.233, 418.273, 436.283
Cer	36:1	$C_{36}H_{71}NO_3Cl$	600.513	600.513	<1	NA
FA	22:6	$C_{22}H_{31}O_2$	327.233	327.233	<1	229.195, 283.243,

						309.174
	20:4	$C_{20}H_{31}O_2$	303.233	303.233	<1	205.195, 259.243, 284.991
	18:0	$C_{18}H_{35}O_2$	283.264	283.264	<1	265.130
	16:0	$C_{16}H_{31}O_2$	255.233	255.233	<1	237.043
N-Acetylaspartic acid		$C_6H_8NO_5$	174.040	174.041	-5.7	58.028, 88.039, 130.049
hexose		$C_6H_{12}O_6Cl$	215.033	215.034	-4.7	NA
glutamate		$C_5H_8NO_4$	146.045	146.046	-6.8	102.054, 128.034
Glutamine		$C_5H_9N_2O_3$	145.061	145.062	-6.9	127.050, 128.034

[a] NA (not available) means that only high mass accuracy was used for tentative ion identification.

Table S2. Data obtained for the identification of selected negative ion mode molecular ions from human thyroid tissue.

Proposed Identification		Proposed formula	Measured *m/z*	Theoretical *m/z*	Mass error (ppm)	Main Fragment ions upon MS/MS[a]
PI	40:5	$C_{49}H_{84}O_{13}P$	911.566	911.566	<1	NA
	38:4	$C_{47}H_{82}O_{13}P$	885.550	885.550	<1	152.994, 223.006, 241.011, 283.264, 303.233, 419.256, 581.310
	36:4	$C_{45}H_{78}O_{13}P$	857.518	857.518	<1	152.994, 241.011, 279.233, 415.226, 577.278
	34:1	$C_{45}H_{80}O_{13}P$	835.534	835.534	<1	152.994, 241.011, 255.232, 391.226, 553.277
PE	38:4	$C_{43}H_{77}NO_8P$	766.539	766.539	<1	140.010, 152.995, 259.243, 283.264, 303.233, 480.309
	36:2	$C_{41}H_{77}NO_8P$	742.539	742.540	-1.3	140.010, 152.994,

						281.248
	P-36:4	$C_{41}H_{73}NO_7P$	722.513	722.513	<1	140.010, 196.037, 259.243, 303.233, 418.270, 436.283
CL	74:7	$C_{83}H_{146}O_{17}P_2$	738.502	738.502	<1	NA
	72:8	$C_{81}H_{140}O_{17}P_2$	723.479	723.479	<1	NA
Cer	34:1	$C_{34}H_{67}NO_3Cl$	572.481	572.482	-1.7	NA
FA	20:4	$C_{20}H_{31}O_2$	303.233	303.233	<1	205.195, 259.243, 284.992
	18:0	$C_{18}H_{35}O_2$	283.265	283.264	3.5	265.130
	18:1	$C_{18}H_{33}O_2$	281.250	281.249	3.6	NA
	18:2	$C_{18}H_{31}O_2$	279.234	279.233	3.6	261.222
	16:0	$C_{18}H_{31}O_2$	255.233	255.233	<1	NA
Ascorbic acid		$C_6H_7O_6$	175.024	175.025	-5.7	87.007, 115.002
Glutamine		$C_5H_9N_2O_3$	145.050	145.062	-8.3	NA
I-			126.904	126.905	-7.9	NA

[a] NA (not available) means that only high mass accuracy was used for tentative ion identification.

Table S3. Data obtained for the identification of selected negative ion mode molecular ions from human ovarian tissue.

Proposed Identification		Proposed formula	Measured *m/z*	Theoretical *m/z*	Mass error (ppm)	Main Fragment ions upon MS/MS[a]
PI	40:4	$C_{49}H_{86}O_{13}P$	913.581	913.581	<1	223.000, 241.011, 283.264, 331.264, 419.257, 581.309
	38:4	$C_{47}H_{82}O_{13}P$	885.549	885.550	-1.1	152.994, 223.000, 241.011, 283.264, 303.233, 419.256, 439.225, 581.309
	36:1	$C_{45}H_{84}O_{13}P$	863.565	863.566	-1.2	152.995, 241.011, 281.248, 283.264,

						419.256
	34:1	$C_{43}H_{80}O_{13}P$	835.534	835.534	<1	152.994, 223.000, 241.011, 255.233, 281.248, 391.225, 553.278
PS	38:3	$C_{44}H_{79}NO_{10}P$	812.544	812.545	-1.2	152.994, 283.264, 305.248, 419.256, 437.266, 725.514
	36:1	$C_{42}H_{79}NO_{10}P$	788.545	788.545	<1	281.248, 283.264, 417.242, 419.256, 437.268, 701.512
PE	38:4	$C_{43}H_{80}O_{13}P$	766.539	766.539	<1	259.243, 283.264, 303.233, 480.309
	O-38:5	$C_{43}H_{77}NO_7P$	750.544	750.544	<1	259.243, 303.233, 446.303, 464.313
	P-35:4	$C_{41}H_{73}NO_7P$	722.512	722.513	-1.4	259.243, 303.233, 418.273, 436.283
FA	16:0	$C_{16}H_{31}O_2$	255.232	255.233	-3.9	NA
Ascorbic acid		$C_6H_7O_6$	175.024	175.024	<1	87.007, 115.002

[a] NA (not available) means that only high mass accuracy was used for tentative ion identification.

Table S4. Data obtained for the identification of selected negative ion mode molecular ions from human lung tissue.

Proposed Identification		Proposed formula	Measured *m/z*	Theoretical *m/z*	Mass error (ppm)	Main Fragment ions upon MS/MS[a]
PI	40:4	$C_{49}H_{86}O_{13}P$	913.580	913.581	-1.1	152.994, 223.000, 241.010, 283.264, 331.264, 419.256, 581.311
	38:4	$C_{47}H_{82}O_{13}P$	885.550	885.550	<1	152.994, 223.000, 241.011, 283.264, 303.233, 419.256, 581.311
	36:1	$C_{45}H_{84}O_{13}P$	863.565	863.566	-1.2	152.994, 241.011, 281.248, 283.264, 419.256, 581.311
	36:2	$C_{45}H_{82}O_{13}P$	861.548	861.549	-1.2	152.994, 223.000, 241.011, 281.256, 417.241
PG	36:2	$C_{42}H_{78}O_{10}P$	773.542	773.534	10	152.994, 281.256, 417.241, 491.278, 509.288
	34:1	$C_{40}H_{76}O_{10}P$	747.514	747.517	-4.0	152.994, 255.233, 281.256, 391.226, 417.241, 491.277
PE	38:4	$C_{43}H_{77}NO_8P$	766.535	766.539	-5.2	140.010, 283.256, 303.233, 480.309,
	36:1	$C_{41}H_{79}NO_8P$	744.552	744.555	-4.0	140.011, 281.256, 283.264, 480.307

	P-38:4	$C_{43}H_{77}NO_7P$	750.534	750.544	-13	259.243, 303.233, 464.314
	P-36:4	$C_{41}H_{73}NO_7P$	722.511	722.513	-2.8	259.243, 303.233, 418.273, 436.283
	O-34:2	$C_{39}H_{75}NO_7P$	700.527	700.529	-2.9	NA
Cer	34:1	$C_{34}H_{67}NO_3Cl$	572.479	572.482	-5.2	NA
FA	18:1	$C_{18}H_{33}O_2$	281.249	281.249	<1	NA
Ascorbic Acid		$C_6H_7O_6$	175.023	175.024	-5.7	115.002

[a] NA (not available) means that only high mass accuracy was used for tentative ion identification.

Table S5. Data obtained for the identification of selected negative ion mode molecular ions from human breast tissue.

Proposed Identification		**Proposed formula**	**Measured *m/z***	**Theoretical *m/z***	**Mass error (ppm)**	**Main Fragment ions upon MS/MS[a]**
PI	38:4	$C_{47}H_{82}O_{13}P$	885.550	885.550	<1	152.994, 223.000, 241.011, 283.264, 303.233, 419.257, 581.310, 599.319
	36:1	$C_{45}H_{84}O_{13}P$	863.565	863.566	-1.2	152.994, 223.000, 241.011, 281.248, 283.264, 419.256, 581.309
PG	36:2	$C_{42}H_{78}O_{10}P$	773.542	773.534	10	152.994, 281.248, 417.240, 491.276
FA	20:4	$C_{20}H_{31}O_2$	303.233	303.233	<1	205.195, 259.243, 284.991
	18:1	$C_{18}H_{33}O_2$	281.249	281.249	<1	NA

[a] NA (not available) means that only high mass accuracy was used for tentative ion identification.

Table S6. Patient demographics of the 253 human tissue samples used in this study.

Patient Diagnosis		Median age, Years	Age range, Years	Number of patients by gender (male, female)	Number of patients by race (White, Black, Asian, Unknown)
Breast	Normal	47	24-76	(0, 29)	(21, 7, 1, 0)
	Cancer	58	41-75	(2, 14)	(10, 2, 4, 0)
Lung	Normal	57	12-82	(33, 14)	(35, 12, 0, 0)
	Cancer	66	22-84	(25, 23)	(35, 7, 0, 6)
Ovary	Normal	50	31-80	(0, 29)	(22, 7, 0, 0)
	Cancer	62	30-83	(0, 28)	(25, 2, 0, 1)
Thyroid	Normal	40	18-80	(10, 17)	(18, 7, 0, 2)
	Tumor	49	16-81	(12, 17)	(21, 4, 0, 4)

Movie S1. Simulation demonstrating the use of the MasSpec Pen for routine intraoperative diagnosis.